doi:10.1016/j.jmb.2011.12.040 J. Mol. Biol. (2012) 416, 414–424

Contents lists available at www.sciencedirect.com

Journal of Molecular Biology

journal homepage: http://ees.elsevier.com.jmb

The Carboxy-Terminal Third of Dystrophin Enhances Actin Binding Activity

Davin M. Henderson, Ava Yun Lin, David D. Thomas and James M. Ervasti*

Department of Biochemistry, Molecular Biology, and Biophysics, University of Minnesota, Minneapolis, MN 55455, USA

Received 7 September 2011; received in revised form 19 December 2011; accepted 20 December 2011
Available online 28 December 2011

Edited by R. Craig

Keywords:
dystrophin;
actin binding protein;
actin dynamics;
cooperative binding;
muscular dystrophy

Dystrophin is an actin binding protein that is thought to stabilize the cardiac and skeletal muscle cell membranes during contraction. Here, we investigated the contributions of each dystrophin domain to actin binding function. Cosedimentation assays and pyrene–actin fluorescence experiments confirmed that a fragment spanning two-thirds of the dystrophin molecule [from N-terminal actin binding domain (ABD) 1 through ABD2] bound actin filaments with high affinity and protected filaments from forced depolymerization, but was less effective in both assays than full-length dystrophin. While a construct encoding the C-terminal third of dystrophin displayed no specific actin binding activity or competition with full-length dystrophin, our data show that it confers an unexpected regulation of actin binding by the N-terminal two-thirds of dystrophin when present in cis. Time-resolved phosphorescence anisotropy experiments demonstrated that the presence of the C-terminal third of dystrophin in cis also influences actin interaction by restricting actin rotational amplitude. We propose that the C-terminal region of dystrophin allosterically stabilizes an optimal actin binding conformation of dystrophin.

Introduction

Dystrophin is an essential component of the dystrophin–glycoprotein complex that functions to protect the muscle cell membrane from contraction-induced injury.[1] The dystrophin–glycoprotein complex is localized to a lattice-like structure in muscle, called the costamere, that is thought to transmit force radially from the z-disc to neighboring muscle fibers.[2–5] Dystrophin is a multidomain protein with two globular domains at its N-terminus and C-terminus that are connected by a large rod domain consisting of 24 spectrin-like repeats with four interspersed hinge regions.[6,7] The C-terminal domain of dystrophin encodes a WW domain, a ZZ domain, and two EF hand domains that interact with the cytoplasmic tail of β-dystroglycan.[8–12] Dystrophin interacts with actin filaments at two sites: at actin binding domain (ABD) 1 at its N-terminus, which is composed of a tandem calponin homology domain,[13,14] and at ABD2 within spectrin-like repeats 11–17, which interacts with actin filaments via electrostatic attraction.[15] Through the concerted actions of these two distinct binding interactions, dystrophin is thought to physically anchor the sarcolemma to the costameric actin cytoskeleton, thereby stabilizing the membrane against mechanical damage during muscle use. A

*Corresponding author. 6-155 Jackson Hall, 321 Church Street SE, Minneapolis, MN 55455, USA. E-mail address: jervasti@umn.edu.

Abbreviations used: ABD, actin binding domain; TPA, time-resolved phosphorescence anisotropy; SEM, standard error of the mean; ErIA, erythrosine iodoacetamide; NIH, National Institutes of Health.

recent biophysical characterization of dystrophin–actin interaction showed that binding of full-length dystrophin restricts actin microsecond rotational amplitude but increases the rate.[16] This paradoxical combination is novel to dystrophin and utrophin,[16] and is hypothesized to effect a strong but resilient dystrophin–actin interaction to prevent contraction-induced damage.

Here, we have systematically measured the specific contributions of each dystrophin domain to its actin binding function through actin cosedimentation, depolymerization, and time-resolved phosphorescence anisotropy (TPA) assays. While the extent of actin binding to dystrophin constructs can be evaluated through actin cosedimentation assays and depolymerization assays, these measurements provide no information about the physical properties of the bound complex. TPA provides a direct measure of the structural dynamics of the bound complex.[16] We have established through previous TPA studies that full-length dystrophin restricts actin rotational amplitude but increases the rate, and we proposed that these effects are important for the stability and resilience of the dystrophin–actin complex at the subsarcolemmal region.[16] Our binding assays demonstrate that large fragments containing a single tested ABD showed similar affinities for actin as isolated ABDs. Most interestingly, while the C-terminal third of dystrophin displayed no measurable affinity for actin, or competition with full-length dystrophin binding to actin, our data suggest a regulatory function for the C-terminal domain in the stabilization of a dystrophin conformation that binds actin with maximal affinity. In addition, we demonstrate through TPA assays that the C-terminal domain can impact the regulation of actin rotational dynamics (i.e., flexibility) by the ABDs of dystrophin.

Results

Dystrophin domain contributions

Several previous studies from our laboratory reported the affinities of the dystrophin N-terminal ABD1,[17] the middle rod ABD2,[18] ABD1 plus spectrin repeats 1–10,[19] or both ABD1 and ABD2 linked by spectrin repeats 1–10.[19] Here, we directly compared the affinities of two previously studied constructs (DysN-R10 and Dys N-R17), as well as ABD2, in the context of the DP260 isoform of dystrophin to determine whether the small unique N-terminus of DP260 or whether the presumed actin nonbinding C-terminal third of dystrophin influences actin binding affinity (Fig. 1). We also measured the actin binding affinity of a therapeutically relevant miniaturized dystrophin protein[20] that retains ABD1 and the C-terminus but lacks ABD2 (DysΔH2-R19). Because the dystrophin constructs exhibited variable degrees of concentration-dependent self-pelleting, we varied the concentration of actin in our cosedimentation assay around a fixed concentration of the dystrophin construct (0.5 μM). Varying the actin concentration is advantageous because any self-pelleting protein can be easily subtracted from the protein that cosediments with actin filaments.[21] DP260 bound actin filaments with a K_d of 6.85 ± 4.62 μM (Fig. 2a), in good agreement with previously published data (7.3 μM) for isolated ABD2.[18] These results suggest that neither the unique N-terminus of DP260 nor the C-terminal region influences the actin binding affinity of ABD2. DysΔH2-R19 and DysN-R10 bound to actin filaments with approximately an order-of-magnitude lower affinity compared to the full-length protein, with K_d values of 3.53 ± 1.73 μM for DysΔH2-R19 (Fig. 2c) and 3.92 ± 2.18 μM for DysN-R10 (Fig. 2b) *versus* a K_d of 0.11 ± 0.0082 μM for dystrophin (Fig. 2e). These

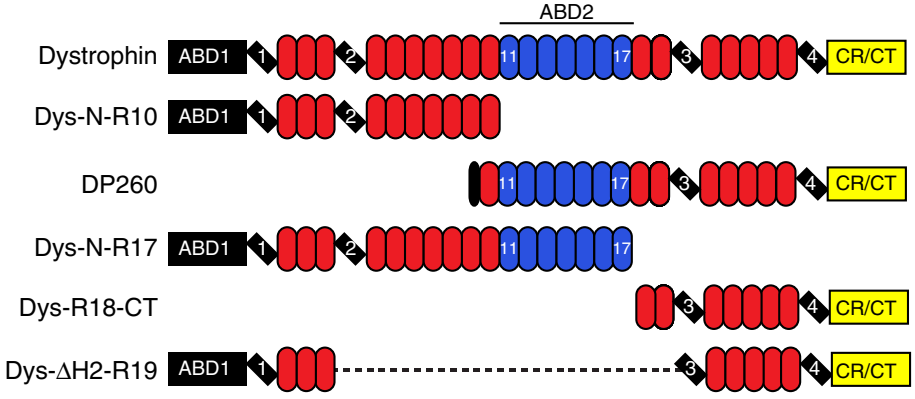

Fig. 1. Domain map of proteins assayed. Globular N-terminal and C-terminal domains are represented by rectangles. Hinge regions are marked by tilted rectangles. Spectrin-like repeats are represented by ovals and shown in blue for actin binding repeats. Non-actin-binding spectrin-like repeats are shown in red.

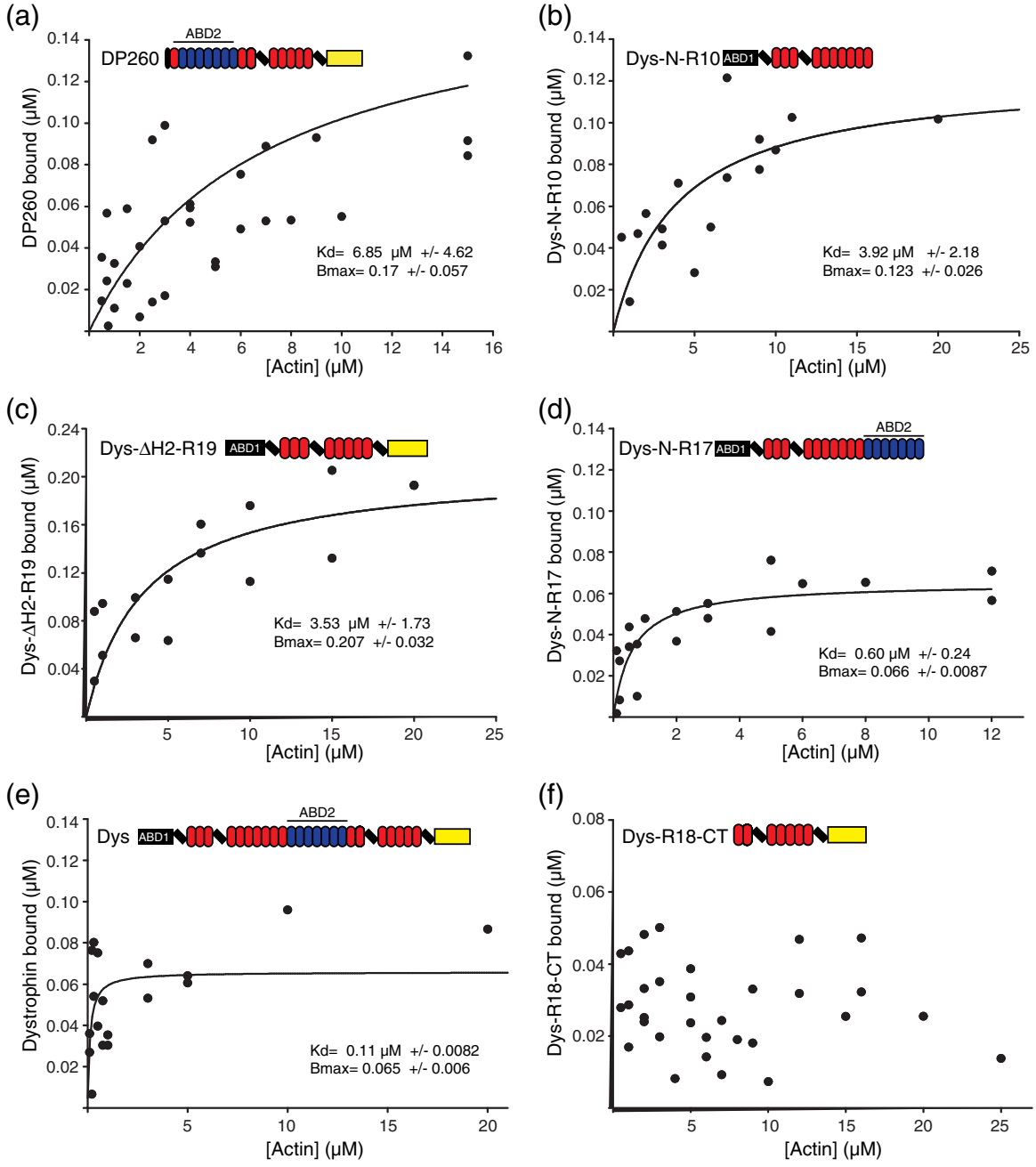

Fig. 2. Analysis of dystrophin ABDs. Binding isotherms from actin cosedimentation assays with increasing actin concentrations and constant concentrations of DP260 (a), DysN-R10 (b), DysΔH2-R19 (c), DysN-R17 (d), full-length dystrophin (e), and DysR18-CT (f). Plots on each graph display the results from at least three independent experiments. Binding curves were fitted with regression analysis to determine K_d and B_{max} (inset) values. The color code for domain diagrams is the same as in that in Fig. 1.

data confirm that two ABDs need to be in cis to achieve the submicromolar binding affinity measured for full-length dystrophin.[15,19]

Interestingly, comparison of data for DysN-R17 (Fig. 2d) with data for dystrophin (Fig. 2e) suggested that the C-terminal third of dystrophin may contribute to enhanced actin binding affinity. By fitting the aggregate data from three independent binding experiments to a hyperbola, we measured a K_d of 0.6 ± 0.24 μM and a B_{max} of 0.066 ± 0.0087 for DysN-R17 (Fig. 2d) compared to a K_d of 0.11 ± 0.0082 μM and a B_{max} of 0.065 ± 0.006 for dystrophin (Fig. 2e). To determine if the actin binding affinities of dystrophin and DysN-R17 were significantly different, we

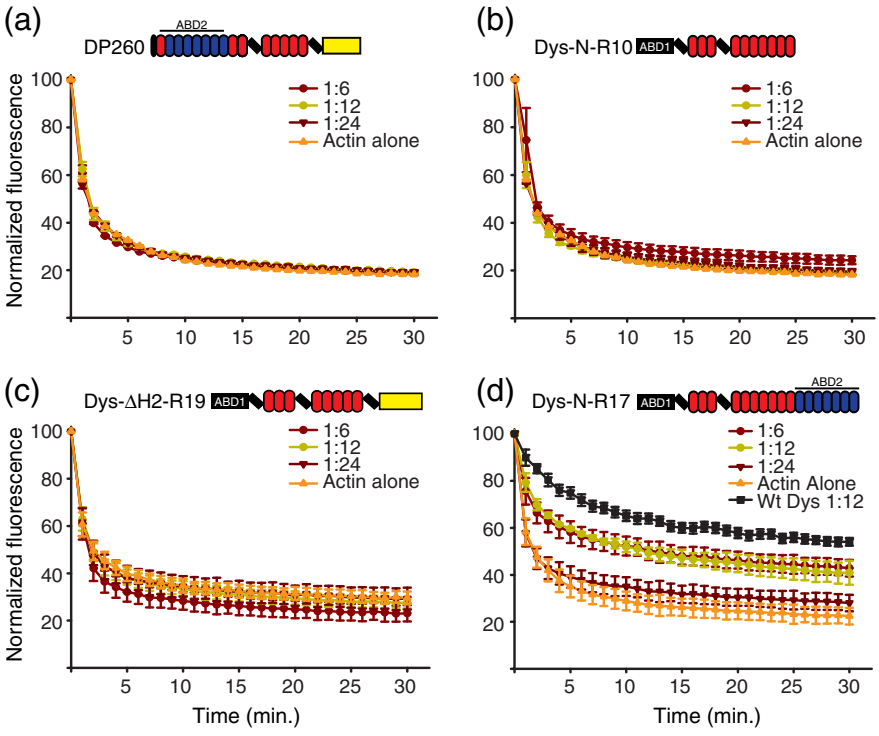

Fig. 3. Actin depolymerization protection analysis of dystrophin fragments. Actin depolymerization was monitored by measuring the decay of pyrene–actin fluorescence after dilution into a low-salt buffer below the critical concentration. Actin was measured alone or in the presence of dystrophin/actin molar ratios of 1:6, 1:12, and 1:24 for DysN-R10 (a), DP260 (b), Dys-ΔH2-R19 (c), and DysN-R17 (d). (a–d) Error bars represent SEM. The black curve in (d) represents values from full-length dystrophin measured previously.[21]

computed for K_d values from curve fits to each individual binding experiment and values averaged for each construct. By this method, the mean K_d for DysN-R17 was 0.553 ± 0.118 μM [standard error of the mean (SEM)]. The mean K_d for dystrophin was 0.152 ± 0.124 μM, which was significantly different from that of DysN-R17 by Student's *t* test ($p = 0.0063$). DysN-R17 and full-length dystrophin were previously shown to bind with apparent K_d values of 0.76 μM and 0.3 μM, respectively, but using an assay design where their concentrations were varied around a fixed actin concentration.[19] While the relative difference in actin binding affinities between DysN-R17 and dystrophin is consistent between our current study and our previous study,[19] we suggest that self-association at high DysN-R17 concentrations increased error around the measurements previously reported to obscure significance.

Although their similar actin binding stoichiometries suggest that DysN-R17 encodes the full ABD of dystrophin, the significantly lower affinity of DysN-R17 compared with full-length dystrophin suggests that the C-terminal third of dystrophin may play a role in actin binding. However, an isolated C-terminal fragment encoding spectrin repeat 18 through the C-terminus of dystrophin (DysR18-CT) showed only nonspecific binding to actin filaments up to a concentration of 25 μM actin (Fig. 2f).

To further address whether DysN-R17 binds actin filaments with lower affinity than full-length dystrophin, we measured the ability of each protein to protect actin filaments from forced depolymerization.[19] Consistent with previous studies,[22,23] none of the large dystrophin fragments containing only ABD1 or ABD2 (DP260, DysN-R10, and DysΔH2-R19) was able to protect actin filaments from forced depolymerization, confirming that both ABD1 and ABD2 must be present in cis to afford protection (Fig. 3a–c). DysN-R17 significantly protected actin filaments from depolymerization, albeit with reduced capacity compared to the full-length protein, further suggesting that the C-terminal region enhances actin binding activity (Fig. 3d).

Effect of the C-terminal region of dystrophin on actin binding

Although DysR18-CT exhibited no measurable actin binding activity (Fig. 2f), DysN-R17 exhibited a significantly lower affinity compared to full-length dystrophin. Therefore, we hypothesized that the actin nonbinding C-terminal third of dystrophin may facilitate a cooperative interaction between adjacent dystrophin molecules docked on an actin filament, analogous to the cooperative model of actin binding in tropomyosin.[24] To test if DysR18-CT may participate in actin binding through a head-to-tail association with a second dystrophin molecule, we assayed the ability of DysR18-CT to inhibit the binding of full-length dystrophin to actin filaments. However, increasing concentrations of DysR18-CT had no measurable effect on dystrophin's affinity for

actin, as measured in both high-speed cosedimentation assay (Fig. 4a and b) and forced depolymerization assay (Fig. 4c and d).

Dystrophin domain contributions to actin dynamics

We recently demonstrated that dystrophin binding affects the torsional flexibility of actin filaments.[16] To test for the possible effects of the dystrophin C-terminal region on actin torsional flexibility, we performed TPA to compare the effects of dystrophin constructs with and without the C-terminal region on actin dynamics. TPA was performed with erythrosine iodoacetamide (ErIA) coupled to Cys374 of each actin protomer, and the degree of filament anisotropy (orientational order) was measured as a function of time after excitation with a pulsed laser. From the calculated anisotropy decays, the amplitudes and rates corresponding to the filament bending and twisting motions of actin (Fig. 5a) were calculated.[25] We previously demonstrated that the dystrophin–actin complex is characterized by a paradoxical combination of a restriction in actin rotational amplitude and an increase in rate.[16] Additionally, our previous TPA studies[16] showed a cooperative restriction of actin rotational amplitude and an increase in rotational rate when full-length dystrophin was bound (Fig. 5b and c, red). In contrast, DysN-R17 lost functional cooperativity as its titration caused a linear decrease in the angular amplitude of actin rotational motion (Fig. 5b, blue), corresponding to a drop in the degree of cooperativity (n) from 9.6 to 1.3 when compared with full-length dystrophin (Fig. 5d and e, blue). Loss of the C-terminal region from DysN-R17 also ablated the effect on rate observed with full-length dystrophin (Fig. 5c, blue). These results suggest that the decreased protection of DysN-R17 against actin depolymerization was also the result of an altered mode of interaction between the ABDs and actin.

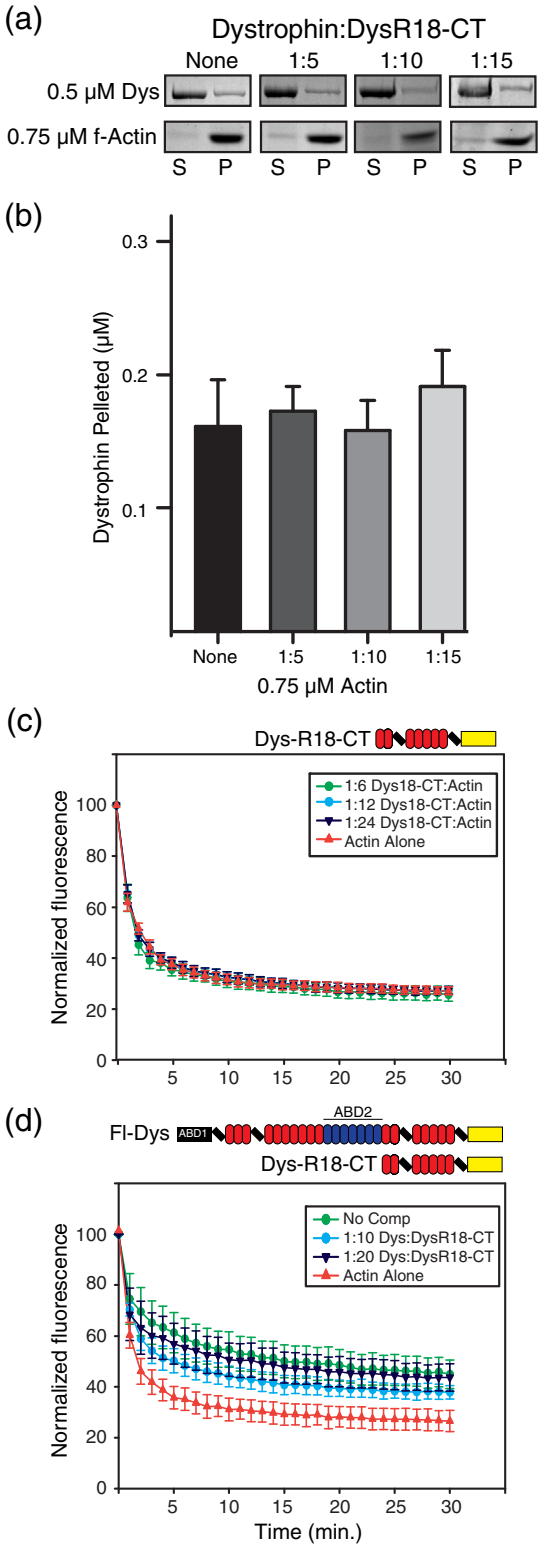

Fig. 4. Dystrophin C-terminus competition. (a) A single-point dystrophin–actin cosedimentation assay with a fixed actin concentration of 0.75 μM and a dystrophin concentration of 0.5 μM. DysR18-CT was added at dystrophin/DysR18-CT molar ratios of 1:5, 1:10, and 1:15 to compete for full-length dystrophin binding. Boxed images are Coomassie-stained polyacrylamide gels that display the amounts of dystrophin and actin in the supernatant and pellet for each ratio of DysR18-CT added. (b) Bar graph depicting the quantitation of the cosedimentation assay in (a). No significant difference in actin binding activity is observed with increasing amounts of DysR18-CT. (c) Actin depolymerization protection control experiment at DysR18-CT/actin molar ratios of 1:6, 1:12, and 1:24. (d) Actin depolymerization protection assay with full-length dystrophin alone at a dystrophin/actin molar ratio of 1:12, and DysR18-CT added as a competitor at dystrophin/DysR18-CT molar ratios of 1:10 and 1:20. No significant competition was observed for the amounts of DysR18-CT tested. (b–d) Error bars represent SEM.

Despite its lower affinity and lack of protection in depolymerization assays, DP260 showed a dramatic rescue of the cooperative effect in restricting actin rotational amplitude in TPA (Fig. 5b, green), increasing the degree of cooperativity to that observed in full-length dystrophin at 9.8 (Fig. 5d and e, green). However, DP260 failed to increase actin rotational rate (Fig. 5c, green). These results suggest that the C-terminal region allosterically influences ABD2 to restrict actin rotational amplitude, but both ABDs and the C-terminal region appear to be necessary to increase the rotational rate.

Despite the high sensitivity of the TPA assay to changes in actin dynamics, a large range of DysR18-CT (0.3 –13.5 μM) to ErIA actin (1 μM) concentrations had no significant effect on actin rotational motion (Fig. 6a and b). The effect on actin rotational amplitude (Fig. 6a) or rate (Fig. 6b) was minimal and mostly within the range of ErIA actin alone. The occasional outlier showed, at most, a 15% change in

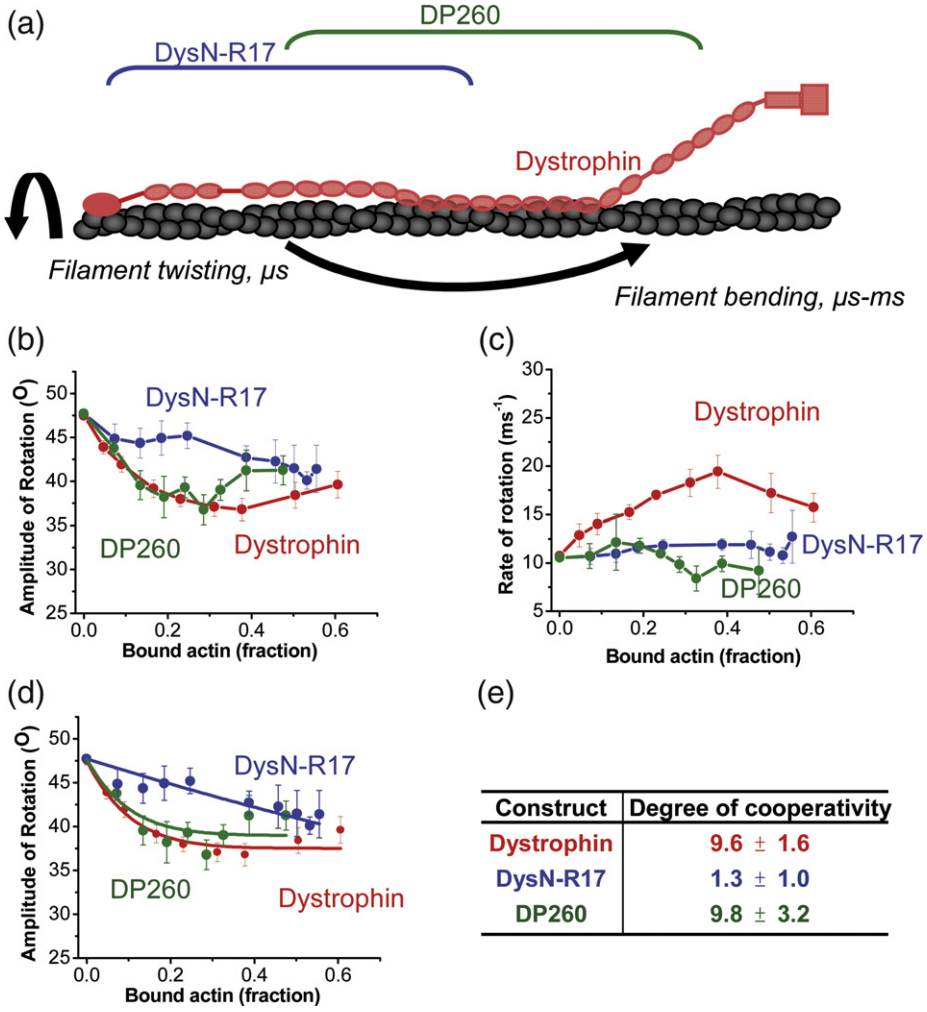

Construct	Degree of cooperativity
Dystrophin	9.6 ± 1.6
DysN-R17	1.3 ± 1.0
DP260	9.8 ± 3.2

Fig. 5. TPA shows that the C-terminal region of dystrophin contributes to the cooperative restriction of actin rotational amplitude. (a) Diagram of actin rotational dynamics evaluated by TPA when bound to full-length dystrophin (red), DysN-R17 (blue), or DP260 (green). Effects on the amplitudes (b) and rates (c) of actin rotational motion are plotted against the fraction of bound actin protomers (Eq. (5)). Full-length dystrophin (red) restricts the amplitude and increases the rate of actin rotational motion.[16] Deletion of the C-terminal region of dystrophin in DysN-R17 (blue) shows a similar restriction of amplitude (b) at higher titrations compared with full-length dystrophin, but there is loss in the cooperativity of the effect. DP260 (green) containing the C-terminal tail regains the cooperative effect on restricting actin rotational amplitude. However, the loss of the C-terminal or N-terminal regions in either DysN-R17 or DP260 fails to produce any increase in the rate of rotational motion in actin (c). The degree of cooperativity n was determined by fitting to the equilibrium binding constant (Eq. (5)) (d) and summarized in (e). The results from the fits in (d) show that DysN-R17 loses considerable cooperativity in its effect on the rotational amplitude of actin filaments compared with dystrophin. On the other hand, DP260 with the C-terminal region intact restores the degree of cooperativity seen in full-length dystrophin in restricting the angular amplitude of rotational motion.

actin rotational amplitude and a 6% change in rate, which are quite minimal compared to the average 26% and 80% changes, respectively, observed when dystrophin was bound to actin (Fig. 5a and b, red dotted lines). The TPA results are congruent with both cosedimentation data and actin depolymerization data. We conclude that the C-terminal third of dystrophin neither directly participates in actin binding nor enhances binding through a head-to-tail interaction with neighboring dystrophin molecules (analogous to the tropomyosin model[24]), but its presence in cis with ABD1 and ABD2 enhances the ability of dystrophin to bind and regulate actin filament dynamics.

Discussion

It has been well established by multiple studies that dystrophin binds actin filaments with submicromolar affinity through the concerted actions of ABD1 and ABD2.[15,18,19] While previous studies have measured the actin binding properties of ABD1 and ABD2 in isolation and reported ~10-fold lower affinities than measured for full-length dystrophin, our study is the first to directly compare the properties of ABD1, ABD2, and the C-terminal third of dystrophin with full-length protein (Fig. 2). We found that large constructs containing only one ABD (DP260, DysN-R10, and DysΔH2-R19) exhibited actin binding affinities that matched well with those previously reported for isolated ABD1 and ABD2, and none of these single ABD-containing fragments was able to protect actin filaments against forced depolymerization (Fig. 3). Ablation of one ABD also weakened the effect of dystrophin on actin filament dynamics (Fig. 5, green). Loss of either the N-terminal region in DP260 or the C-terminal region in DysN-R17 eliminated their effect on actin rotational rate (Fig. 5c), although their restriction of rotational amplitude was preserved at higher titrations (Fig. 5b).

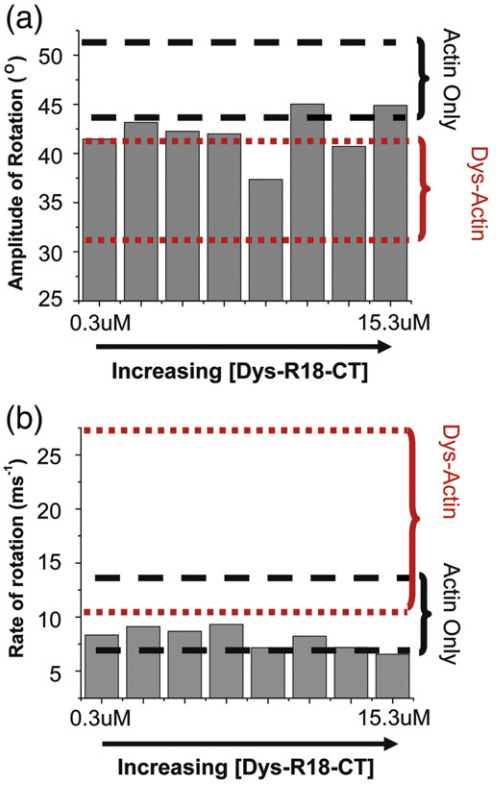

Fig. 6. Lack of specific interaction of the C-terminal region (DysR18-CT) with actin. DysR18-CT has a negligible effect on restricting the amplitude (a) or increasing the rate (b). The ranges of values from actin only (black broken line) and when 40% of the actin is decorated with dystrophin (red dotted line) are shown.

Our binding data demonstrate that DysΔH2-R19 and DP260 have similar affinities for actin filaments *in vitro*, and we previously demonstrated that both DysΔH2-R19 and DP260, when transgenically overexpressed in mdx muscle, can restore the link between the sarcolemma and the costameric cytoskeleton.[26] However, based on differences between DysΔH2-R19 and DP260 in rescuing other dystrophic phenotypes,[27,28] it appears that the N-terminal ABD1 may perform another function in addition to binding actin filaments. DysΔH2-R19, when overexpressed, fully rescued the dystrophic phenotypes of the mdx mouse.[27] In contrast, while DP260 expression prevented contraction-induced injury, it failed to rescue the muscle weakness, necrosis, and regeneration associated with dystrophin deficiency.[28] In support of an actin-independent function for ABD1, the highly homologous ABD of plectin has been shown to differentially bind to actin filaments or integrin cytoplasmic domain dependent on its open-*versus*-closed conformation.[29] Moreover, dystrophin associates with cytokeratins through a direct interaction of keratin 19 with ABD1.[30–32]

While DysN-R17, containing both ABD1 and ABD2, bound actin filaments with similar stoichiometry as full-length dystrophin and significantly protected filaments from depolymerization (Fig. 3d), it bound with significantly lower affinity compared to full-length dystrophin (Fig. 2d). These new data suggest a role for the C-terminal region of dystrophin in increasing actin affinity. However, the isolated C-terminal region (DysR18-CT) exhibited no measurable specific actin binding activity in both cosedimentation assay (Fig. 2f) and forced depolymerization assay (Fig. 4c).

We hypothesize that the dystrophin C-terminal region must be in cis with both ABDs to allosterically influence their binding to actin. We initially thought that the dystrophin–actin interaction may exhibit a head-to-tail cooperative binding similar to the coiled-coil domains of tropomyosin.[24] However, we measured no specific actin binding activity in DysR18-CT (Fig. 2f), and competition experiments

showed that it had no effect on full-length dystrophin binding to actin (Fig. 4). Nevertheless, we cannot rule out a head-to-tail cooperative binding activity, since it may be dependent on the presence of the N-terminal domain.

Additionally, our TPA experiments demonstrate that dystrophin fragments cooperatively restrict actin rotational amplitude only when the C-terminal region is present in the construct (Fig. 5b). The results in Figs. 2f and 4 indicate that dystrophin does not convey cooperative binding similar to that observed in tropomyosin. However, our TPA results indicate that actin rotational amplitude responds cooperatively to dystrophin binding, that this cooperativity is largely dependent on the presence of the C-terminal region, and that the full-length protein is required for increased rotational rate (Fig. 5e). The degree of cooperativity (n) quantifies actin's remarkable allosteric properties in response to different binding partners, which can be as high as several hundreds.[33,34] The high degree of cooperativity observed in the full-length dystrophin–actin complex ($n=9.6$; Fig. 5) could explain why a low amount of expressed dystrophin (29–57%) in humans can prevent the characteristic muscle weakness in muscular dystrophy.[35] It also may explain why expression of 20% dystrophin in transgenic mdx mice (dys null) was sufficient to rescue dystrophic phenotype and that a threshold of only ~5% is enough to partially restore muscle function in *Dko* mice (dys^-/utr^-).[36–38]

Multiple approaches to treating Duchenne muscular dystrophy rely on the deletion of dystrophin domains. Recently, we demonstrated that internal truncation compromises the stability of dystrophin.[20] Our new finding that the C-terminal region of dystrophin influences both actin binding and actin dynamics adds yet another layer of complexity into the design of Duchenne muscular dystrophy therapies but also highlights the potential to biophysically optimize gene therapy constructs prior to extensive testing in animals. For example, inclusion of specific C-terminal spectrin-like repeats in next-generation gene therapy constructs may improve efficacy through enhanced actin binding activity.

Recently, we demonstrated that the isolated C-terminal region (DysR18-CT) exhibits markedly greater thermal stability compared to N-terminal constructs (DysN-R17) or even full-length dystrophin.[20] Since the N-terminal and C-terminal regions of dystrophin have drastically different thermal stabilities (50 °C and 70 °C, respectively), one would expect to observe two melting transitions, but only a single transition exactly halfway in between is instead observed (60 °C). We propose that the highly stable C-terminal third of dystrophin, when present in cis, allosterically influences the N-terminal region of the protein to effect increased thermal stability and to orient or stabilize a conformation required for optimal actin binding. Alternatively, the presence of the N-terminal region in cis with the C-terminal domain may stabilize an actin binding conformation in the C-terminus. Further experiments will be needed to understand how the C-terminal region of dystrophin influences actin binding activity.

Materials and Methods

Cloning, protein expression, and purification

All constructs used for protein expression in this article were previously generated for other studies.[20] Each cDNA was N-terminally Flag tagged using PCR and cloned into either pFastbac1 or pFastbac duel downstream of the polyhedrin promoter. Once in pFastbac, bacmids were generated using the Bac-to-Bac system (Invitrogen). A high-titer virus was used to infect Sf21 insect cells at a density of between 1.0 cells/ml and 1.5×10^6 cells/ml, with a volume of 250 ml. Proteins were purified by Flag affinity chromatography and dialyzed against two changes of phosphate-buffered saline (pH 7.5) to remove excess Flag peptide. Proteins were concentrated in Millipore Amicon Ultra centrifuge-based concentrators with a cutoff of either 100 kDa or 10 kDa, depending on protein molecular mass.

Actin cosedimentation assays

In actin cosedimentation assays, the concentration of actin, instead of dystrophin, was varied identically to Henderson *et al.*[21] Each reaction was incubated at room temperature for 30 min and centrifuged at 100,000*g* for 30 min. The resulting supernatant and pellet fractions were subjected to SDS-PAGE and stained with Coomassie blue. The supernatant and pellet fractions were determined by densitometry with UVP analysis software. The concentration of actin was varied between 0.1 μM and 25 μM, and the concentration of dystrophin or dystrophin fragment was fixed at 0.5 μM. Additionally, the fraction of dystrophin protein found to pellet without actin was quantitated by densitometry from Coomassie-stained gels, and the self-pelleting fraction was subtracted from subsequent reactions where actin was present. Three independent experiments were performed for each dystrophin protein, and the aggregate data were plotted and fitted using nonlinear regression analysis identically to Rybakova *et al.*[19] and Henderson *et al.*[21] A single ligand binding site equation was used in Sigma Plot (Systat Software) for nonlinear regression.

Actin depolymerization assays

Depolymerization protection assays were performed with pyrene-labeled actin from the cytoskeleton, as previously described.[21] In short, pyrene-labeled actin at 2 μM was incubated with dystrophin or dystrophin fragments at a dystrophin/actin ratio of 1:6, 1:12, or 1:24. Actin was forced to depolymerize by dilution below the critical concentration with G-buffer [10 mM Tris (pH 8.0) and 2 mM $CaCl_2$]. Samples were immediately read on a Gemini (Molecular Devices) fluorescence plate reader every minute for 30 min.

C-Terminal competition experiments

Dystrophin–actin binding was performed as described above at a near-K_d concentration of 0.75 μM actin and incubated with increasing concentrations of DysR18-CT (1:5, 1:10, and 1:15). Results were compiled by analyzing the scanned Coomassie-stained gel by densitometry and plotted as a bar graph. Student's t test was used to determine significance. Actin depolymerization protection assays were performed as described above, except that DysR18-CT was added at dystrophin/DysR18-CT ratios of 1:10 and 1:20 to a reaction containing full-length dystrophin at a dystrophin/actin monomer ratio of 1:2.

Time-resolved phosphorescence anisotropy

Actin preparation and labeling with phosphorescent ErIA (Anaspec) were performed as described by Prochniewicz *et al.*[16] Phalloidin-stabilized ErIA actin was diluted in U/D buffer [100 mM $NaCl_2$, 2 mM $MgCl_2$, 0.2 mM ATP, 1 mM DTT, and 10 mM Tris (pH 7.5)] to 1 μM. Increasing concentrations of dystrophin and fragments (Fig. 1) were added to 1 μM ErIA actin. An oxygen-removing system containing glucose oxidase (55 μg/ml), catalase (36 μg/ml), and glucose (45 μg/ml) was added to the sample prior to each experiment to maximize the phosphorescence signal.[39,40] The phosphorescent dye was excited at 532 nm with a vertically polarized 1. 2-ns laser pulse from an FDSS 532-150 laser (CryLas) with a 100-Hz repetition rate. Emission was detected through a 670-nm glass cutoff filter (Corion) using a photomultiplier (R928; Hamamatsu) and a transient digitizer (CompuScope 14100; GaGe) with a resolution of 1 μs/channel. Time-resolved anisotropy is defined by:

$$R(t) = \frac{I_v(t) - GI_h(t)}{I_v(t) + 2GI_h(t)} \quad (1)$$

where $I_v(t)$ and $I_h(t)$ are defined by the vertical and horizontal components of the detected phosphorescent emission, using a single detector at 90° and a rotating sheet polarizer alternating between the two orientations every 500 laser pulses. The instrument response function G was calibrated by detecting the signal with a horizontally polarized excitation pulse and correcting it so that the anisotropy is 0. All time-resolved anisotropy experiments were recorded with 30 cycles, with 500 pulses each in the horizontal and vertical planes.

The anisotropy decays were analyzed by fitting to the function:

$$r(t) = r_1\exp(-t/\phi_1) + r_2\exp(-t/\phi_2) + r_\infty \quad (2)$$

where rotational correlation times ϕ_1 (slow) and ϕ_2 (fast) and amplitudes r_1, r_2, and r_∞ were varied using a least-squares minimization procedure.[41] Results were validated by a comparison of the residuals and chi-squares of the fits at one, two, and three exponential terms. Increase in final anisotropy r_∞ indicates a decrease in the amplitudes of microsecond rotational dynamics, which is attributed to a decrease in actin filament flexibility. A maximally flexible molecule (isotropic) would exhibit a final anisotropy value of 0. The slower motions (ϕ_1,r_1) represent mainly actin filament bending, while the faster motions (ϕ_2,r_2) represent mainly actin filament twisting. The combined rates of the filament twisting and bending motions were evaluated by ϕ_{ave}, which is calculated by a weighted average of ϕ_1 and ϕ_2. The overall angular amplitudes of the microsecond motions in actin were calculated using the wobble-in-a-cone model:[25]

$$\theta_c(\mu s) = \cos^{-1}\left[-0.5 + \sqrt{0.5\left(1 + 8\sqrt{r_\infty / r_0}\right)}\right] \quad (3)$$

This reflects the combined amplitude of microsecond filament bending and twisting motions depicted in Fig. 6a.

The rates of the corresponding angular amplitudes were calculated by:

$$\text{rate}\left(\mu s^{-1}\right) = 1 / \phi_{ave} \quad (4)$$

Graphs of the amplitude and the rate of actin rotation dynamics are plotted against the fractional saturation of protein-decorated actin (fraction-bound actin).[16] This is different from the cosedimentation plots, since the goal of this assay is not to evaluate the degree of binding but to measure the structural effects of the bound state. Cosedimentation assays using a fixed concentration of ErIA (6 μM) binding to varied concentrations of dystrophin constructs were performed to obtain K_d and Y_{max} values. These values were then used to calculate the fraction of actin bound to dystrophin constructs in our TPA assays using the quadratic equation:

$$y = \frac{Y_{max}(x + P_t + K_d) - \sqrt{(x + P_t + K_d) - 4xP_t}}{2P_t} \quad (5)$$

where y is the fractional saturation of actin by bound dystrophin construct (mol/mol actin), and x is the added concentration of the dystrophin construct. P_t is defined as the concentration of available binding sites for the dystrophin construct, which is [actin]Y_{max}. The fraction of bound actin is then calculated by y/Y_{max}.

The degree of cooperativity is determined by fitting the plot of angular amplitudes θ_∞ (Eq. (2)) *versus* the fraction of actin decorated with dystrophin or dystrophin constructs to the equilibrium binding equations:[34]

$$\theta_{c(OBS)} = \theta_c(\theta_c - \theta_a)(1-v)^n \quad (6)$$

where $\theta_{c(OBS)}$ is the observed amplitude, θ_a is the amplitude of actin only, and θ_∞ is the amplitude of the actin bound to dystrophin or related constructs listed in Fig. 1. The parameter v is the fraction of actin decorated with dystrophin or related constructs, and n is the degree of cooperativity in the system (i.e., the number of unbound actin monomers affected by a single monomer binding to dystrophin).

Acknowledgements

We thank Bin Li for excellent technical support. This work was supported by the National Institutes of Health (NIH) Training Program in Muscle

Research (AR007612), NIH grant RO1 AR042423 to J.M.E., NIH grant R01 AG026160 to D.D.T., and NIH grant F30 AG034033 to A.Y.L. TPA experiments were performed in the Biophysical Spectroscopy Facility supported by NIH grant P30 AR057220.

References

1. Ervasti, J. M. & Sonnemann, K. J. (2008). Biology of the striated muscle dystrophin–glycoprotein complex. *Int. Rev. Cytol.* **265**, 191–225.
2. Porter, G. A., Dmytrenko, G. M., Winkelmann, J. C. & Bloch, R. J. (1992). Dystrophin colocalizes with beta-spectrin in distinct subsarcolemmal domains in mammalian skeletal muscle. *J. Cell Biol.* **117**, 997–1005.
3. Straub, V., Bittner, R. E., Leger, J. J. & Voit, T. (1992). Direct visualization of the dystrophin network on skeletal muscle fiber membrane. *J. Cell Biol.* **119**, 1183–1191.
4. Ervasti, J. M. (2003). Costameres: the Achilles' heel of Herculean muscle. *J. Biol. Chem.* **278**, 13591–13594.
5. Zubrzycka-Gaarn, E. E., Bulman, D. E., Karpati, G., Burghes, A. H., Belfall, B., Klamut, H. J. *et al.* (1988). The Duchenne muscular dystrophy gene product is localized in sarcolemma of human skeletal muscle. *Nature*, **333**, 466–469.
6. Koenig, M., Monaco, A. P. & Kunkel, L. M. (1988). The complete sequence of dystrophin predicts a rod-shaped cytoskeletal protein. *Cell*, **53**, 219–228.
7. Koenig, M. & Kunkel, L. M. (1990). Detailed analysis of the repeat domain of dystrophin reveals four potential hinge segments that may confer flexibility. *J. Biol. Chem.* **265**, 4560–4566.
8. Ishikawa-Sakurai, M., Yoshida, M., Imamura, M., Davies, K. E. & Ozawa, E. (2004). ZZ domain is essentially required for the physiological binding of dystrophin and utrophin to beta-dystroglycan. *Hum. Mol. Genet.* **13**, 693–702.
9. Ponting, C. P., Blake, D. J., Davies, K. E., Kendrick-Jones, J. & Winder, S. J. (1996). ZZ and TAZ: new putative zinc fingers in dystrophin and other proteins. *Trends Biochem. Sci.* **21**, 11–13.
10. Hnia, K., Zouiten, D., Cantel, S., Chazalette, D., Hugon, G., Fehrentz, J. A. *et al.* (2007). ZZ domain of dystrophin and utrophin: topology and mapping of a beta-dystroglycan interaction site. *Biochem. J.* **401**, 667–677.
11. Bork, P. & Sudol, M. (1994). The WW domain: a signalling site in dystrophin? *Trends Biochem. Sci.* **19**, 531–533.
12. Rentschler, S., Linn, H., Deininger, K., Bedford, M. T., Espanel, X. & Sudol, M. (1999). The WW domain of dystrophin requires EF-hands region to interact with beta-dystroglycan. *Biol. Chem.* **380**, 431–442.
13. Levine, B. A., Moir, A. J., Patchell, V. B. & Perry, S. V. (1990). The interaction of actin with dystrophin. *FEBS Lett.* **263**, 159–162.
14. Way, M., Pope, B., Cross, R. A., Kendrick-Jones, J. & Weeds, A. G. (1992). Expression of the N-terminal domain of dystrophin in *E. coli* and demonstration of binding to F-actin. *FEBS Lett.* **301**, 243–245.
15. Amann, K. J., Renley, B. A. & Ervasti, J. M. (1998). A cluster of basic repeats in the dystrophin rod domain binds F-actin through an electrostatic interaction. *J. Biol. Chem.* **273**, 28419–28423.
16. Prochniewicz, E., Henderson, D., Ervasti, J. M. & Thomas, D. D. (2009). Dystrophin and utrophin have distinct effects on the structural dynamics of actin. *Proc. Natl Acad. Sci. USA*, **106**, 7822–7827.
17. Renley, B. A., Rybakova, I. N., Amann, K. J. & Ervasti, J. M. (1998). Dystrophin binding to nonmuscle actin. *Cell Motil. Cytoskeleton*, **41**, 264–270.
18. Amann, K. J., Guo, A. W. & Ervasti, J. M. (1999). Utrophin lacks the rod domain actin binding activity of dystrophin. *J. Biol. Chem.* **274**, 35375–35380.
19. Rybakova, I. N., Humston, J. L., Sonnemann, K. J. & Ervasti, J. M. (2006). Dystrophin and utrophin bind actin through distinct modes of contact. *J. Biol. Chem.* **281**, 9996–10001.
20. Henderson, D. M., Belanto, J. J., Li, B., Heun-Johnson, H. & Ervasti, J. M. (2011). Internal deletion compromises the stability of dystrophin. *Hum. Mol. Genet.* **20**, 2955–2963.
21. Henderson, D. M., Lee, A. & Ervasti, J. M. (2010). Disease-causing missense mutations in actin binding domain 1 of dystrophin induce thermodynamic instability and protein aggregation. *Proc. Natl Acad. Sci. USA*, **107**, 9632–9637.
22. Rybakova, I. N., Amann, K. J. & Ervasti, J. M. (1996). A new model for the interaction of dystrophin with F-actin. *J. Cell Biol.* **135**, 661–672.
23. Rybakova, I. N. & Ervasti, J. M. (1997). Dystrophin–glycoprotein complex is monomeric and stabilizes actin filaments *in vitro* through a lateral association. *J. Biol. Chem.* **272**, 28771–28778.
24. Tobacman, L. S. (2008). Cooperative binding of tropomyosin to actin. *Adv. Exp. Med. Biol.* **644**, 85–94.
25. Prochniewicz, E., Zhang, Q., Howard, E. C. & Thomas, D. D. (1996). Microsecond rotational dynamics of actin: spectroscopic detection and theoretical simulation. *J. Mol. Biol.* **255**, 446–457.
26. Hanft, L. M., Rybakova, I. N., Patel, J. R., Rafael-Fortney, J. A. & Ervasti, J. M. (2006). Cytoplasmic gamma-actin contributes to a compensatory remodeling response in dystrophin-deficient muscle. *Proc. Natl Acad. Sci. USA*, **103**, 5385–5390.
27. Harper, S. Q., Hauser, M. A., DelloRusso, C., Duan, D., Crawford, R. W., Phelps, S. F. *et al.* (2002). Modular flexibility of dystrophin: implications for gene therapy of Duchenne muscular dystrophy. *Nat. Med.* **8**, 253–261.
28. Warner, L. E., DelloRusso, C., Crawford, R. W., Rybakova, I. N., Patel, J. R., Ervasti, J. M. & Chamberlain, J. S. (2002). Expression of Dp260 in muscle tethers the actin cytoskeleton to the dystrophin–glycoprotein complex and partially prevents dystrophy. *Hum. Mol. Genet.* **11**, 1095–1105.
29. Garcia-Alvarez, B., Bobkov, A., Sonnenberg, A. & de Pereda, J. M. (2003). Structural and functional analysis of the actin binding domain of plectin suggests alternative mechanisms for binding to F-actin and integrin beta4. *Structure*, **11**, 615–625.
30. O'Neill, A., Williams, M. W., Resneck, W. G., Milner, D. J., Capetanaki, Y. & Bloch, R. J. (2002). Sarcolemmal organization in skeletal muscle lacking desmin: evidence for cytokeratins associated with the membrane skeleton at costameres. *Mol. Biol. Cell*, **13**, 2347–2359.

31. Ursitti, J. A., Lee, P. C., Resneck, W. G., McNally, M. M., Bowman, A. L., O'Neill, A. *et al.* (2004). Cloning and characterization of cytokeratins 8 and 19 in adult rat striated muscle. Interaction with the dystrophin glycoprotein complex. *J. Biol. Chem.* **279**, 41830–41838.
32. Stone, M. R., O'Neill, A., Catino, D. & Bloch, R. J. (2005). Specific interaction of the actin-binding domain of dystrophin with intermediate filaments containing keratin 19. *Mol. Biol. Cell*, **16**, 4280–4293.
33. Prochniewicz, E., Zhang, Q., Janmey, P. A. & Thomas, D. D. (1996). Cooperativity in F-actin: binding of gelsolin at the barbed end affects structure and dynamics of the whole filament. *J. Mol. Biol.* **260**, 756–766.
34. Prochniewicz, E., Janson, N., Thomas, D. D. & De la Cruz, E. M. (2005). Cofilin increases the torsional flexibility and dynamics of actin filaments. *J. Mol. Biol.* **353**, 990–1000.
35. Neri, M., Torelli, S., Brown, S., Ugo, I., Sabatelli, P., Merlini, L. *et al.* (2007). Dystrophin levels as low as 30% are sufficient to avoid muscular dystrophy in the human. *Neuromuscular Disord.* **17**, 913–918.
36. Wells, D. J., Wells, K. E., Asante, E. A., Turner, G., Sunada, Y., Campbell, K. P. *et al.* (1995). Expression of human full-length and minidystrophin in transgenic mdx mice: implications for gene therapy of Duchenne muscular dystrophy. *Hum. Mol. Genet.* **4**, 1245–1250.
37. Phelps, S. F., Hauser, M. A., Cole, N. M., Rafael, J. A., Hinkle, R. T., Faulkner, J. A. & Chamberlain, J. S. (1995). Expression of full-length and truncated dystrophin mini-genes in transgenic mdx mice. *Hum. Mol. Genet.* **4**, 1251–1258.
38. Li, D., Yue, Y. & Duan, D. (2010). Marginal level dystrophin expression improves clinical outcome in a strain of dystrophin/utrophin double knockout mice. *PLoS One*, **5**, e15286.
39. Prochniewicz, E., Walseth, T. F. & Thomas, D. D. (2004). Structural dynamics of actin during active interaction with myosin: different effects of weakly and strongly bound myosin heads. *Biochemistry*, **43**, 10642–10652.
40. Eads, T. M., Thomas, D. D. & Austin, R. H. (1984). Microsecond rotational motions of eosin-labeled myosin measured by time-resolved anisotropy of absorption and phosphorescence. *J. Mol. Biol.* **179**, 55–81.
41. Prochniewicz, E. & Thomas, D. D. (1997). Perturbations of functional interactions with myosin induce long-range allosteric and cooperative structural changes in actin. *Biochemistry*, **36**, 12845–12853.